Phys. Status Solidi A **206**, No. 5, 952–955 (2009) / **DOI** 10.1002/pssa.200881307

physica status solidi a
www.pss-a.com
applications and materials science

Ensemble effect on Rabi oscillations of excitons in quantum dots

Mamiko Kujiraoka[*, 1, 2], **Junko Ishi-Hayase**[**, 1, 3, 4], **Kouichi Akahane**[1], **Naokatsu Yamamoto**[1], **Kazuhiro Ema**[2], **and Masahide Sasaki**[1]

[1] National Institute of Information and Communications Technology, 4-2-1 Nukui-Kitamachi, Koganei, Tokyo 184-8795, Japan
[2] Department of Physics, Sophia University, 7-1 Kioi-cho, Chiyoda-ku, Tokyo 102-8554, Japan
[3] PRESTO, Japan Science and Technology Agency (JST), 4-1-8 Honcho, Kawaguchi, Saitama 332-0012, Japan
[4] The University of Electro-Communications, 1-5-1 Chofugaoka, Chofu, Tokyo 182-8585, Japan

Received 11 August 2008, revised 21 November 2008, accepted 23 November 2008
Published online 23 April 2009

PACS 71.35.–y, 78.47.jf, 78.47.nj, 78.67.Hc

[*] Corresponding author: e-mail m-kujira@nict.go.jp, Phone: +81 42 327 5264, Fax: +81 42 327 6629
[**] e-mail j-hayase@pc.uec.ac.jp, Phone: +81 42 443 5920, Fax: +81 42 443 5920

We observed excitonic Rabi oscillations (ROs) in quantum dots (QDs) by four-wave mixing (FWM) and pump-probe techniques. When a large number of QDs are excited by a spatially nonuniform laser, the inhomogeneous distribution of the transition dipole moments of the QD excitons and the spatial distribution of the input electric field induce distribution of the Rabi frequencies. We investigated this ensemble effect on the ROs of the excitonic polarization and the excitonic population observed in the FWM and pump-probe signals. By calculating the FWM and pump-probe signals including the Gaussian distribution of the pulse area, we first showed that a part of the ensemble effect can be cancelled out only in case of the ROs of the excitonic polarization. This reflects the differences between the characteristics of excitonic polarization and population.

1 Introduction Optical Rabi oscillations (ROs) in two-level systems play crucial roles in processing and storing quantum information [1–3]. Excitonic states in semiconductor quantum dots (QDs) have been attractive candidates for the demonstration of ROs in solid-state structures because they are approximately identified as two-level systems and they maintain their coherence for a long time. In a QD, time-integrated ROs are usually observed as sinusoidal oscillations of excitonic population or excitonic polarization with respect to the area of the excitation pulse. However, most of the reported excitonic ROs showed significant deviation from the ideal two-level ROs; for example, strong damping of the oscillation amplitude and modulation of the oscillation period with an increase in the pulse area [1]. The reasons for the deviation observed in single QDs include the excitation-induced dephasing effect [4], biexciton effect [5] and local-field effect [6, 7]. Strong damping is expected in ROs occurring in a macroscopic number of QDs excited by a spatially nonuniform laser, mainly owing to the ensemble effect, i.e. the pulse area distribution for each QD with an exciton; this distribution is attributed to the inhomogeneous distribution of the exciton transition dipole moments and the spatial distribution of the input electric field. Strong damping of the ROs of excitonic population caused by the distribution of the transition dipole moments was reported in an InGaAs QD ensemble [1]. However, the ensemble effect on the ROs of excitonic polarization has never been studied so far. Moreover, there is no report on the comparison of ROs of excitonic polarization with those of the excitonic population in QDs.

Recently, we observed the ROs of excitonic polarization in strain-compensated InAs QDs using a four-wave mixing (FWM) technique [8] but did not discuss the ensemble effect. In this study, we measured the ROs of the excitonic population by a pump-probe technique in the same QD sample and compared the ensemble effect on the ROs of the excitonic population with those of the excitonic polarization. We calculated the FWM and pump-probe signals by taking into account the Gaussian distribution of the pulse area in order to investigate the ensemble effect.

2 Experiment The sample was fabricated using molecular beam epitaxy; it contained 150 layers of InAs self-assembled QDs embedded in 60-nm-thick $In_{0.52}Ga_{0.1}Al_{0.38}As$ spacers on an InP(311)B substrate [9]. Our QDs are elliptical in shape and are elongated in the [$\bar{2}$33] direction which is one of the crystal axes on the (311)B surface. The back side of our sample was anti-reflection coated to prevent multiple reflections. The sample was fabricated using strain compensation to control the emission wavelength and to stack 150 QD layers without degrading the crystalline quality. The corresponding effective QD density was $\sim 1 \times 10^{13}$ dots/cm^2. The highly stacked structure of our sample is an advantage for enhancing weak nonlinear signals that are measured to observe excitonic ROs under resonant excitation [8]. We recently found that the ground-state excitons in our QDs showed an extremely long dephasing time due to the negligible pure dephasing and non-radiative population relaxation [10, 11]. Therefore, our strain-compensated QDs are suitable for the investigation of excitonic ROs.

Two-pulse FWM and pump-probe techniques were used to investigate the ROs of the excitonic polarization and population, respectively. Excitation was performed using 1.1-ps optical pulses generated by a Ti:sapphire-pumped optical parametric oscillator at a repetition rate of 76 MHz. We measured the FWM intensity $|\boldsymbol{P}_{\mathrm{FWM}}|^2$ in the $2\boldsymbol{k}_2 - \boldsymbol{k}_1$ direction and the differential transmission (DT) of the probe pulse as a function of the average area of pulse 1, $\bar{\Theta}_1$, as schematically shown in Fig. 1.

The time delay between two excitation pulses was fixed at 20 ps in all the measurements. Since both the pulse duration ΔT and the time delay were considerably shorter than the dephasing time and the population relaxation time (>1 ns) [10, 11], we can ignore the relaxation processes in the present experiment.

The average pulse area $\bar{\Theta}_i$ which was calculated using the equation $\bar{\Theta}_i = \bar{\mu}\bar{E}_i\,\Delta T/\hbar$, was changed by changing the average excitation intensity $\bar{I}_i$, while maintaining the temporal profile of the excitation pulse constant. Here, we assume a rectangular pulse with a time duration of ΔT. $\bar{\mu}$ and $\bar{E}_i$ represent the average transition dipole moment of the excitons and the average electric field, respectively. $\bar{E}_i$ is defined by the relation $\bar{E}_i^2 \propto \bar{I}_i \propto \langle I_i \rangle/(\pi R^2)$, where $\langle I_i \rangle$ represents the spatially integrated excitation intensity measured in front of the sample using a power meter. R (~60 μm) corresponds to the beam radius estimated by fit

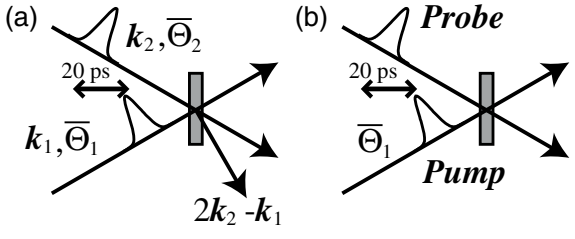

Figure 1 Experimental arrangements of (a) FWM and (b) pump–probe techniques.

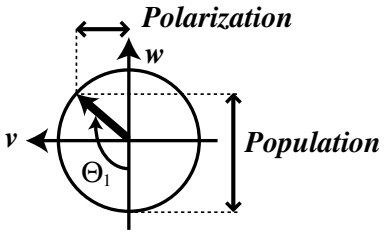

Figure 2 Bloch sphere for a two-level system. Excitonic population is proportional to $\sin^2(\Theta_1/2)$ and excitonic polarization is proportional to $\sin\Theta_1$.

ting the spatial profile of the excitation pulses on the sample surface to the Gaussian function. $\bar{\mu}$ was estimated to be 58 Debye from the average radiative lifetime (1.01 ns) [11]. Thus, $\bar{\Theta}_i$ was determined to be independent of the observed FWM and pump–probe signals.

The wavelength of the excitation pulses was tuned to 1468 nm to resonantly excite the ground states of the excitons. Due to the narrow pulse bandwidth, only 3% of 10^9 QDs in the beam spot were resonantly excited. The polarization direction of $\boldsymbol{k}_1$, $\boldsymbol{k}_2$ in the FWM measurements and that of the pump pulse in the pump-probe measurements were aligned in the [$\bar{2}$33] direction in order to selectively excite one of the two nondegenerate exciton ground states [11]. The excitation density of the probe pulse was set at 0.4 nJ/cm^2/pulse in order to read out the excitonic population excited by the pump pulse. The polarization direction of the probe pulse was perpendicular to that of the pump pulse in order to cut off the pump pulse by a polarizer in front of the detector. All the measurements were performed at 3 K.

In an ideal two-level system, the Bloch vector rotates from the lower to the upper state with an increase in the pulse area, according to the optical Bloch equations, as shown in Fig. 2.

In the case of excitonic ROs, the upper state is equivalent to the exciton ground state, and the lower state is equivalent to the crystal ground state, where no exciton exists in a QD. The excitonic polarization corresponding to the value of $\boldsymbol{v}$ is proportional to $\sin\Theta_1$, while the excitonic population corresponding to the value of $\boldsymbol{w}$ is proportional to $\sin^2(\Theta_1/2)$. Therefore, the amplitude of the FWM signals observed in the arrangement shown in Fig. 1(a) is described by $\boldsymbol{P}_{\mathrm{FWM}} \propto \sin\Theta_1 \sin^2(\Theta_2/2)$ [12], while the DT intensity observed in the arrangement shown in Fig. 1(b) is described by $\mathrm{DT} \propto \sin^2(\Theta_1/2)$. By changing Θ_1, we expect to observe the ROs of excitonic polarization (population), which are consistent with the above-mentioned equations.

3 Results and discussion Figure 3(a) shows the change in the FWM signal intensity as a function of $\bar{\Theta}_1$ at 3 K. $\bar{\Theta}_2$ was fixed to π in this study. The closed circles represent the observed signals, and the dashed line represents the theoretical curve for the ideal two-level system, $|\boldsymbol{P}_{\mathrm{FWM}}|^2 \propto \sin^2\bar{\Theta}_1$. The observed FWM intensity shows a clear oscillatory behaviour. Surprisingly, the experimental

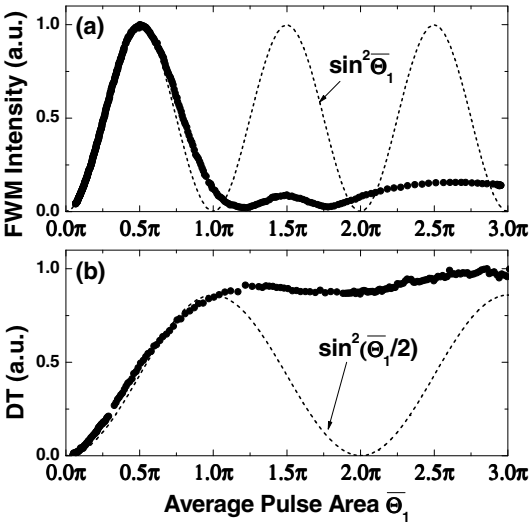

Figure 3 Observed (a) FWM intensity and (b) differential transmission as a function of average pulse area. The dashed lines represent the theoretical curves for an ideal two-level system.

result was almost consistent with $\sin^2 \bar{\Theta}_1$ at $\bar{\Theta}_1 < \pi$, although we did not use any fitting parameters without the oscillator amplitude. Even in the region with large $\bar{\Theta}_1$, the signal decreased to zero at around $n\pi$ (n = 1, 2), and a second peak is observed at around $\bar{\Theta}_1 = 1.5\pi$, although the amplitude is strongly damped.

Figure 3(b) shows the DT signals as a function of $\bar{\Theta}_1$ at 3 K. The closed circles show the observed signals, and the dashed line corresponds to theoretical curve, DT $\propto \sin^2 (\bar{\Theta}_1/2)$. The observed DT reached its maximum at around $\bar{\Theta}_1 = \pi$, though it did not decrease with a further increase in $\bar{\Theta}_1$. The oscillatory behaviour was hardly observed in the region with large $\bar{\Theta}_1$. This behaviour is markedly different from that of the FWM signals.

The differences between the FWM and pump-probe signals can be well explained by the pulse area distribution. In this experiment, the focused beam is spatially distributed as a Gaussian function with a radius of 60 μm. As many as 10^8 dots in the laser spot are simultaneously excited under resonance. Therefore, the QDs in the beam spot are excited not by the same electric field strength but by different field strengths depending on their positions. This results in spatial distribution of the electric field for each QD at each different position. In addition, each QD may have an intrinsic exciton transition dipole moment. These effects lead to a pulse area distribution for each QD, which is referred to as the ensemble effect in this study.

We calculated the FWM intensity and DT as a function of $\bar{\Theta}_1$ by assuming a two-dimensional Gaussian distribution function of $\bar{\Theta}_i$ shown in Fig. 4.

The maximum pulse area $\Theta_i(0,0)$ equals $\sqrt{2}\,\bar{\Theta}_i$, where $\bar{\Theta}_i$ corresponds to the average pulse area used in the experiments. We performed integration from $x, y = -\infty$ to ∞ corresponding to the ensemble average of various ROs.

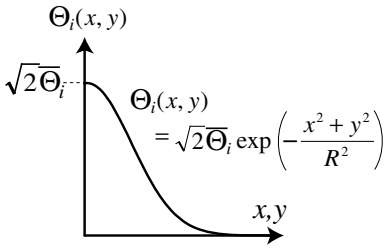

Figure 4 Distribution function of pulse area $\bar{\Theta}_1$.

Figure 5 shows the results of the calculation for the (a) FWM signals and (b) DT signals. The solid lines represent the ensemble average of the signals for different pulse areas. The calculations reproduce the experimental value very well, although any fitting parameter without the oscillation amplitude was not used. For the DT signals, the integration smears out the oscillation structures of $\sin^2 (\bar{\Theta}_1/2)$ owing to the superposition of $\sin^2 (\Theta_1(x, y)/2)$ with different $\Theta_1(x, y)$. On the other hand, in the case of the FWM signals, integration did not smear out the oscillation of $\sin \bar{\Theta}_1$, i.e. the intensity peaked at around $\bar{\Theta}_1 = \pi/2$ and decreased to zero at around $\bar{\Theta}_1 = n\pi$ (n = 1, 2). This feature is considerably different from the DT signal. The reasons for this difference are as follows: since the integration in the FWM signals involves the superposition of $\sin \Theta_1(x, y) \sin^2 (\Theta_2(x, y)/2)$, which have both positive and negative values, the ensemble effect is partly cancelled out in the integration. The compensation of the ensemble effect becomes most effective at around $n\pi$, where the direction of excitonic polarization changes. As a result, the FWM signal intensity decreases to zero at around $n\pi$, and

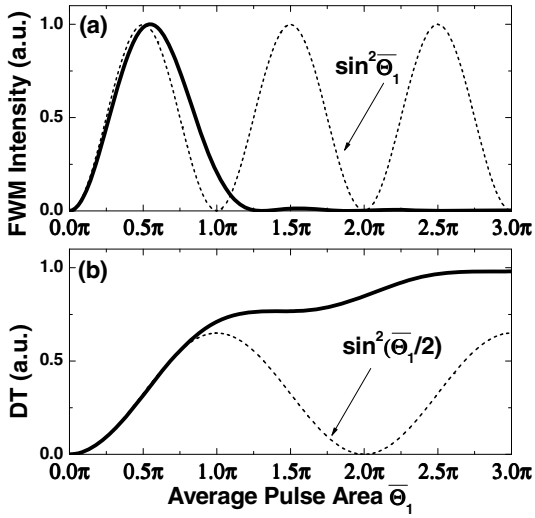

Figure 5 Numerical calculation of (a) FWM intensity and (b) differential transmission as a function of pulse area $\bar{\Theta}_1$. The dashed lines represent the theoretical curves for the ideal two-level system and the solid lines represent the theoretical curve considering the distribution of the pulse area.

the oscillatory behaviour is retained in a few cycles. These features are clearly seen in the observed FWM signal. The good agreement between the experimental results and the calculation without any many-body effects confirmed that those effects can be ignored in the present experiment.

4 Conclusions We observed excitonic ROs from a macroscopic number of QDs using FWM and pump-probe and investigated the ensemble effects on the ROs of excitonic polarization and population. By calculating the FWM and pump-probe signals including the pulse area distribution, we first showed that a part of the ensemble effect was cancelled out only in case of the ROs observed in the FWM signals. This phenomenon is attributed to the differences in the characteristics between the excitonic population and excitonic polarization.

References

[1] P. Borri, W. Langbein, S. Schneider, U. Woggon, R. L. Sellin, D. Ouyang, and D. Bimberg, Phys. Rev. B **66**, 081306R (2002).
[2] T. H. Stievater, X. Li, D. G. Steel, D. Gammon, D. S. Katzer, D. Park, C. Piermarocchi, and L. J. Sham, Phys. Rev. Lett. **87**, 133603 (2001).
[3] H. Kamada, H. Gotoh, J. Temmyo, T. Takagahara, and H. Ando, Phys. Rev. Lett. **87**, 246401 (2001).
[4] Q. Q. Wang, A. Muller, P. Bianucci, E. Rossi, Q. K. Xue, T. Takagahara, C. Piermarocchi, A. H. MacDonald, and C. K. Shih, Phys. Rev. B **72**, 035306 (2005).
[5] B. Patton, U. Woggon, and W. Langbein, Phys. Rev. Lett. **95**, 266401 (2005).
[6] Y. Mitsumori, A. Hasegawa, M. Sasaki, H. Maruki, and F. Minami, Phys. Rev. B **71**, 233305 (2005).
[7] G. Ya. Slepyan, A. Magyarov, S. A. Maksimenko, A. Hoffmann, and D. Bimberg, Phys. Rev. B **70**, 045320 (2004).
[8] J. Ishi-Hayase, K. Akahane, Y. Yamamoto, M. Kujiraoka, K. Ema, and M. Sasaki, J. Lumin. **128**, 1016 (2008).
[9] K. Akahane, N. Ohtani, Y. Okada, and M. Kawabe, J. Cryst. Growth **245**, 31 (2002).
[10] J. Ishi-Hayase, K. Akahane, N. Yamamoto, M. Sasaki, M. Kujiraoka, and K. Ema, Appl. Phys. Lett. **91**, 103111 (2007).
[11] M. Kujiraoka, J. Ishi-Hayase, K. Akahane, Y. Yamamoto, K. Ema, and M. Sasaki, J. Lumin. **128**, 972 (2008).
[12] I. Abram, Phys. Rev. B **40**, 5460 (1989).